DOI 10.5012/bkcs.2011.32.6.2051

Evaluation of Toxicity and Gene Expression Changes Triggered by Oxide Nanoparticles

Pooja Dua,[†,‡,a] Kiran N. Chaudhari,[§,a] Chang Han Lee,[†] Nitin K. Chaudhari,[§] Sun Woo Hong,[†] Jong-Sung Yu,[§,*] Soyoun Kim,[‡,*] and Dong-ki Lee[†,*]

[†]*Global Research Laboratory for RNAi Medicine, Department of Chemistry and BK21 School of Chemical Materials Science, Sungkyunkwan University, Suwon 440-746, Korea. [*]E-mail: dklee@skku.edu*
[‡]*Department of Biomedical Engineering, Dongguk University, Seoul 100-715, Korea. [*]E-mail: skim@dongguk.edu*
[§]*Department of Advanced Materials Chemistry, BK21 Research Team, Korea University, Chungnam 339-700, Korea [*]E-mail: jsyu212@korea.ac.kr*
Received January 10, 2011, Accepted April 25, 2011

Several studies have demonstrated that nanoparticles (NPs) have toxic effects on cultured cell lines, yet there are no clear data describing the overall molecular changes induced by NPs currently in use for human applications. In this study, the *in vitro* cytotoxicity of three oxide NPs of around 100 nm size, namely, mesoporous silica (MCM-41), iron oxide (Fe_2O_3-NPs), and zinc oxide (ZnO-NPs), was evaluated in the human embryonic kidney cell line HEK293. Cell viability assays demonstrated that 100 μg/mL MCM-41, 100 μg/mL Fe_2O_3, and 12.5 μg/mL ZnO exhibited 20% reductions in HEK293 cell viability in 24 hrs. DNA microarray analysis was performed on cells treated with these oxide NPs and further validated by real time PCR to understand cytotoxic changes occurring at the molecular level. Microarray analysis of NP-treated cells identified a number of up- and down-regulated genes that were found to be associated with inflammation, stress, and the cell death and defense response. At both the cellular and molecular levels, the toxicity was observed in the following order: ZnO-NPs > Fe_2O_3-NPs > MCM-41. In conclusion, our study provides important information regarding the toxicity of these three commonly used oxide NPs, which should be useful in future biomedical applications of these nanoparticles.

Key Words : MCM-41, Fe_2O_3 nanoparticle, ZnO nanoparticle, HEK293, Microarray

Introduction

Nanoparticles (NPs) have increased surface area to weight ratios relative to the same materials in the non-nano size range. In addition to unusual physical properties, NPs are also more chemically reactive than larger particles, which can be either advantageous or harmful depending on their end use. The nanotech boom started around a decade ago and since then the use of NPs in consumer goods and biomedical applications has dramatically increased. NPs are increasingly applied as drug delivery vehicles, biosensors, imaging contrast reagents, and therapeutic agents. However, it is surprising that even today the scientific and industrial community has no sufficiently clear data on the overall effects of these NPs on human health.

NPs are easily internalized into cells[1,2] and some NPs have even been shown to cross the blood brain barrier[3-5] where they alter biological processes and cause toxicity. Various *in vitro* and *in vivo* studies indicate that some NPs are associated with serious toxicity issues. The most commonly used *in vitro* toxicity tests focus on whether potentially toxic agents result in cell death. However, sublethal cellular changes may also exist that are not visible in such toxicity screens, but may significantly affect biological processes at the organismal level. Hence, it is important to identify overall cellular changes mediated by NP exposure. Identification of molecular signatures of toxicity at the genomic or proteomic levels provides comprehensive and reliable high throughput data. These data can then be used to compare, classify, and grade a NP on a scale of toxicity. In the present study we identified the molecular signatures of toxicity associated with commonly used oxide NPs. We evaluated and compared three NPs, mesoporous silica, iron oxide and zinc oxide (all around 100 nm in size), in terms of toxicity on HEK293 human embryonic kidney fibroblast cells using a cell death assay and DNA microarray analysis. HEK293 cells are well characterized cells, and their relevance as a model for toxicity assessment in humans is well established.[6,7]

Mesoporous silica, due to their large surface areas and easy permeability, has great potential as drug delivery vehicles and biosensors. One of the most commonly used mesoporous silica NPs, MCM-41, contains a hexagonal arrangement of adjustable pore channels. MCM-41 has been shown to exert concentration dependent toxicity on human T cell lymphoma and adenocarcinoma cells, but was not shown to elicit any toxicity or cell differentiation in mesenchymal stem cells.[8-10] Nevertheless, some of the data on MCM-41 cell-based screens were found to be misleading due to the interference of MCM-41 itself with the 2,5-diphenyltetrazolium salt (MTT) used to asses toxicity.[11,12] Iron oxide NPs

[a]These authors contributed equally to this work.

(Fe_2O_3 or Fe_3O_4) have been widely applied as magnetic drug targeting systems[13,14] and contrast agents in magnetic imaging. Cell-based cytotoxicity studies have shown that human mesothelioma cells are sensitive to Fe_2O_3-NPs exposure, but rodent 3T3 cells are non-responsive.[15] In addition, when compared to other metal oxides, naked Fe_2O_3-NPs were found to have no inhibitory effects on human hematopoietic progenitor cell growth[16] and did not induce any inflammatory response in human endothelial cells,[17] but caused marginal toxicity in lung epithelial cells.[18] In view of the present literature, it is difficult to determine whether MCM-41 and Fe_2O_3-NPs are free of associated toxicity, as most of the studies to date have not thoroughly investigated their effects on overall molecular changes occurring in cells.

ZnO-NPs are one of the main constituents of sunscreens due to their UV filtering properties and are also used in the surface coatings of paints, plastics, and textiles to provide antibacterial and antifungal protection. In contrast to mesoporous silica and iron oxide NPs, the use of ZnO-NPs is raising concern as they have been shown to cause significant DNA damage and oxidative stress in a wide range of cell lines tested.[19-21] Therefore, conducting a parallel analysis of cellular and molecular changes in cells exposed to biologically relevant concentrations of MCM-41 and Fe_2O_3 NPs in comparison to ZnO-NPs will provide a better understanding of their toxicity.

Materials and Methods

Cell Culture and Nanoparticle Characterization. HEK293 cells were grown in Dulbecco's Modified Eagle's Medium (DMEM, Invitrogen, Carlsbad, CA, USA) containing 10% fetal bovine serum (Invitrogen) and 1% penicillin and streptomycin. MCM-41 and Fe_2O_3-NPs were prepared as previously published[19-21] and characterized as described in Supplementary Material. Surface morphology and synthesized sample size were examined by scanning electron microscopy (SEM, LEO 1455VP, Hitachi S-4700) at an acceleration voltage of 25 kV. Microscopic features of the samples were observed with a transmission electron microscope (TEM, EM 912 Omega) operated at 120 kV. Total pore volumes were determined from the amount of gas adsorbed at a relative pressure of 0.99. Pore size distribution was derived from the adsorption branches by the Barrett-Joyner-Halenda (BJH) method. Commercially prepared ZnO nanopowder, ≥ 100 nm in size, was obtained from Sigma Aldrich (St. Louis, MO, USA, Cat no: 544906). All the NPs were suspended in phosphate-buffered saline (PBS), sonicated, and immediately applied to HEK293 cells to minimize agglomeration. To further confirm the state of aggregation, NP test concentrations were prepared in DMEM containing 10% FCS and incubated in culture dishes at 37°C under humidified conditions for 24 h. Samples were then charged on grids and TEM images were acquired.

WST-1 Cell Viability Assay. HEK293 cells were seeded in 96-well cell culture plates at a density of 6×10^3 cells per well and incubated with MCM-41, Fe_2O_3 and ZnO NPs at various concentrations in complete DMEM for 24, 48 and 72 h. For each concentration, six replicates were measured. Following incubation, 10 μL of premixed WST-1 reagent (TaKaRa, Bio Inc., Shiga, Japan) were added to each well and further incubated for 2 h. Color development was measured at 450 nm using an ELISA plate reader. All absorbance values were corrected against a blank, which was the same as the test wells except that it was devoid of cells. Percent cell viability was calculated considering the untreated control as 100% viable. The IC_{50} and IC_{20} values were calculated from dose response curves. Cytotoxic effect of nanoparticle-associated ions released in culture medium was also evaluated. Nanoparticles were resuspended in complete medium at indicated concentrations and were incubated for 24, 48 and 72 h, following which the NP suspensions were centrifuged at 13,000 rpm for 10 min and the supernatant medium was collected. HEK293 cells were exposed to the so obtained conditioned medium for various time-points *viz* 24 h in presence of 24 h NP-supernatent, 48h in presence of 48 h NP-supernatent, 72 h in presence of 72 h NP-supernatent .

DNA Microarray. Cells were grown to 60% cell density and treated with 100 μg/mL MCM-41, 100 μg/mL Fe_2O_3, and 12.5 μg/mL ZnO in complete media for 24 h. Total RNA was extracted using the TRI Reagent® kit (Ambion, Austin, TX, USA) according to manufacturer's instructions. Total RNA (10 μg) was used for double-stranded cDNA (dscDNA) synthesis using a commercial kit (Invitrogen). Reactions were stopped with EDTA, treated with RNase A, and the dscDNA was ethanol-precipitated. One μg of dscDNA was used for labeling by Klenow fragments (New England Biolabs, Beverly, MA, USA) using a Cy3-labeled random 9mer (TriLink Biotechnologies, San Diego, CA, USA), and labeled samples were precipitated using isopropanol. Four μg of Cy3-labeled DNA (containing sample tracking control and alignment oligo) was hybridized to a NimbleGen 385K 4-plex human microarray for 18 h at 42 °C using the NimbleGen Hybridization system (Roche NimbleGen Inc., Madison, WI, USA). Arrays were washed and images were obtained using an InnoScan® 900 scanner (Innopsys, Carbonne, France). Scanned images were imported into Mapix software (Innopsys).

Microarray Data Analysis. Scanned images were imported into NimbleScan software. Expression data were normalized through quantile normalization and the Robust Multichip Average (RMA) algorithm.[22] MA plots were generated in which the X-axis represents the average $\log_2$ expression of the control and test samples and the Y-axis corresponds to the ratio of $\log_2$ expression value of the test to the control to visualize overall changes in gene expression. Fold change in expression for 24,000 genes was calculated for each NP relative to the non-treatment control. Transcripts with more than a 2-fold change in either direction were selected. Genes that were differentially expressed by the test materials were functionally categorized using a web-based program, Database for Annotation, Visualization and Integrated Discovery (DAVID) (http://david.abcc.ncifcrf.gov).[23]

Enrichment in gene ontology terms, for both up- and down-regulated genes, was determined by Fisher exact $p < 0.05$ and Count Threshold 2.

Quantitative Real-time PCR. RNA was extracted as described and 500 ng was used as a template for cDNA synthesis, using the High Capacity cDNA Reverse Transcription kit (Applied Biosystems) according to the manufacturer's protocol. Aliquots of the cDNA reaction mixture were analyzed by quantitative real-time PCR using a StepOne real-time PCR thermocycler (Applied Biosystems). Primers used for target specific amplification are shown in Table S2. All primer pairs spanned an intron to avoid possible genomic DNA contamination. The PCR amplification cycle involved denaturation at 95 ºC for 15s, annealing at 60 ºC for 20s, and extension at 72 ºC for 15s. Quantitative real time PCR data for each gene product were normalized by GAPDH transcript levels and are reported as the mean ± SE of relative change compared to the untreated control.

Results and Discussion

Particle Characterization. The MCM-41 particles were spherical in shape and approximately 110 nm in diameter, as shown in SEM and TEM images (Fig. S1). Each particle possessed mesoporous channels running throughout the particle with a pore size of 2.6 nm as indicated by the pore size distribution curve (Fig. S2). The Fe_2O_3 NPs synthesized in this work were demonstrated as hematite α-Fe_2O_3 by XRD pattern as previously published.[21] The SEM image in Figure S1 clearly reveals that the product was composed of a large quantity of uniform hexagonal prism-like α-Fe_2O_3. It was observed from the SEM and TEM images that the Fe_2O_3 sample exhibited a mainly hexagonal nanoplate form with an average parallel side, diagonal side, width, and thickness of 90-100 nm, 60-70 nm, 120-150 nm, and 85-95 nm, respectively. Commercially obtained ZnO nanopowder was ≥ 100 nm in size and had a surface area of 15-25 m^2/g. TEM images of NPs incubated in culture medium for 24 h suggest that no particle agglomeration was observed at 100 μg/mL of MCM-41 and Fe_2O_3 and at 12.5μg/mL ZnO (Figure S3).

Nanoparticle Cytotoxicity on HEK293 Cells. HEK293 cells were exposed to increasing concentrations of test NP materials for 24, 48 and 72 h and cell viability was then measured. All three NPs were earlier shown to be readily internalized into cultured mammalian cells.[8,17] The WST-1 assay is the most sensitive assay available to measure the metabolic activities of viable cells and has the least background interference. Moreover, unlike MTT, WST-1 assay results are not affected by MCM-41-mediated changes in cellular trafficking.[11] Dose response curves clearly show concentration dependent toxicity at all time points (Figure 1). Exposure duration did not significantly affect cell viability at lower MCM-41 and ZnO concentrations; however, at concentrations higher than the IC_{50} the extent of cytotoxicity seemed to correlate with the duration of exposure. IC_{50} values suggest that MCM-41 and Fe_2O_3 had very similar toxicity profiles for 24 and 48 h of incubation. Unlike MCM-41 and Fe_2O_3, ZnO-NPs showed a remarkably steep relationship between ZnO concentration and cell death at concentrations ranging between 15-20 μg/mL, leading to much higher IC_{50} values. A similar concentration dependent

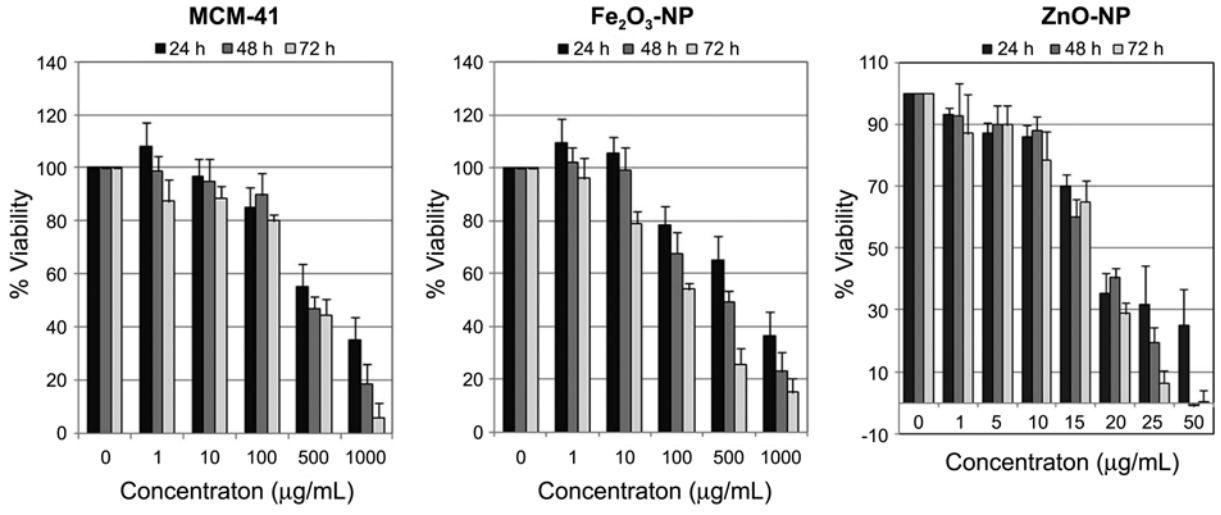

Duration of incubation	MCM-41 (μg/mL)	Fe_2O_3-NP (μg/mL)	ZnO-NP (μg/mL)
24 h	574	698	21.47
48 h	461	464	20.19
72 h	423	116	16.58

Figure 1. Effects of MCM-41, Fe_2O_3-NP, and ZnO-NP on HEK293 cell viability. Cell viability after 24, 48 and 72 h exposure to the test compounds was determined by WST-1 assays. The data are represented as the mean ± SE of three independent experiments and is expressed as percent cell viability with respect to the untreated control as 100% viable. The IC_{50} values of these NPs are given in Table below.

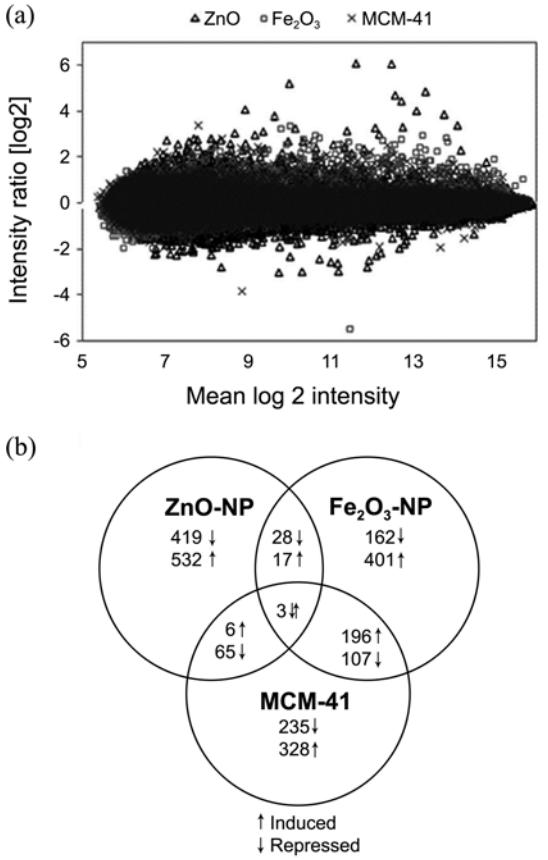

Figure 2. (a) MA Scatter plot showing overall distribution of gene expression upon NP exposure. (b) Venn diagrams illustrating genes induced or repressed by more than 2-fold upon nanoparticle exposure.

response towards ZnO-NPs with a sudden drop in cell viability has been reported in the literature.[19,24] Since metal oxide nanoparticles may be ionized during the sample preparation procedure and the subsequent ion leakage may result in a continuous formation of free radicals and metal ions,[25,26] we also assessed the toxicity imparted due to nanoparticle associated ions. HEK293 cells incubated with NP-conditioned medium suggest that at higher concentrations all the three oxide-NPs resulted in toxicity due to the ions released in the culture medium (Figure S4). Although the contribution of metal ion associated toxicity in MCM41 and Fe_2O_3 seems to fairly low, exposure to ZnO conditioned medium for longer duration resulted in substantial toxicity. Nonetheless, NPs showed much higher cytotoxicity than ions released from NPs for all NPs tested. For further comparative assessment of these NPs, the cell viability assay data was considered as a basis for choosing their equipotent concentrations. Moreover, to make the study more relevant, concentrations were selected that resembled doses at which these NPs are used for human applications. An IC_{20} (concentrations that lead to 20% loss in viability) value for 24 h incubation was considered, as in all three cases, MCM-41 (100 μg/mL)[27,28] Fe_2O_3 (100 μg/mL)[29,30] and ZnO (12.5 μg/mL)[31,32] the concentrations chosen were within the range used for biomedical or other applications.

Nanoparticle Mediated Gene Expression Changes in HEK293 Cells. We performed DNA microarray analysis of HEK293 cells exposed to IC_{20} concentrations of the selected NPs for 24 h to identify the molecular toxicity signature of the oxide NPs under study. The MA plots in Figure 2(a) (average intensity *vs.* intensity ratio) show the overall distributions of gene expression. The number of transcripts that had more than a 2-fold alteration in gene expression in either direction is shown in the Venn diagram (Figure 2(b)). As can be seen, the number and magnitude of genes that were induced were greater in number than those that were repressed. Even at similar cytotoxic concentrations, ZnO-NPs induced greater alterations in gene expression (both number and magnitude) in comparison to the other two test materials. Genes with altered expression and associations with cellular toxicity are listed in Table S1. The genes with altered expression were functionally annotated and the gene ontology (GO) terms with their respective fold-enrichment values were determined (Figure 3(a) and (b)).

Both Fe_2O_3 and MCM-41 induced expressions of many genes that encode for 40S and 60S ribosomal protein homologs. These two NPs also resulted in increased expression of various genes that encode for histones (histone 1, h2ad, h2a, h3 family b) involved in chromatin remodeling. CCL15, a cytokine involved in inflammation and chemotaxis[33] was up-regulated by both MCM-41 and Fe_2O_3. Further gene ontology analysis clearly showed that Fe_2O_3 induced more significant changes than MCM-41. Three genes that are associated with the JNK signaling pathway were up regulated upon Fe_2O_3 exposure (Table S1). JNK signaling is mainly involved in the maintenance of cell viability and proliferation in response to environmental fluctuations and stress.[34] In addition, genes involved in renal system processes, neuron development, and cell proliferation (natriuretic peptide precursor b, endothelin1 and 2, bone morphogenic protein, fibroblast growth factor 8) were also down regulated by Fe_2O_3 but not by MCM-41. Defense response and stress associated genes pregnancy specific beta1 glycoproteins (PSG1 and PSG2)[35] were significantly induced by Fe_2O_3 while only PSG1 was induced by MCM-41.

Unlike MCM-41 and Fe_2O_3 NPs, ZnO-NP resulted in the altered expression of many genes involved in cell death and apoptosis, indicating that even at low concentrations ZnO generates significant toxic responses in the cell. The induced genes included tumor necrosis factor ligands and receptors, interleukin1 beta, interleukin24, von hippel-lindau, somatostatin receptor2, phosphodiesterase7, matrix metalloprotease-9, growth arrest and DNA damage inducible alpha and gamma oncostatin m, protein kinase C gamma, fas apoptotic inhibitory molecule 3, inhibin beta a, and bcl2 like protein. In addition, many genes of the metallothionein family namely MT2a, MT1X, MT1g, MT1b, MT1f showed more than 10-fold induction upon ZnO-NP exposure. Metallothioneins are a family of cysteine rich metal binding proteins that are involved in metal detoxification and in the protection of cells against reactive oxygen species (ROS). In an earlier study,

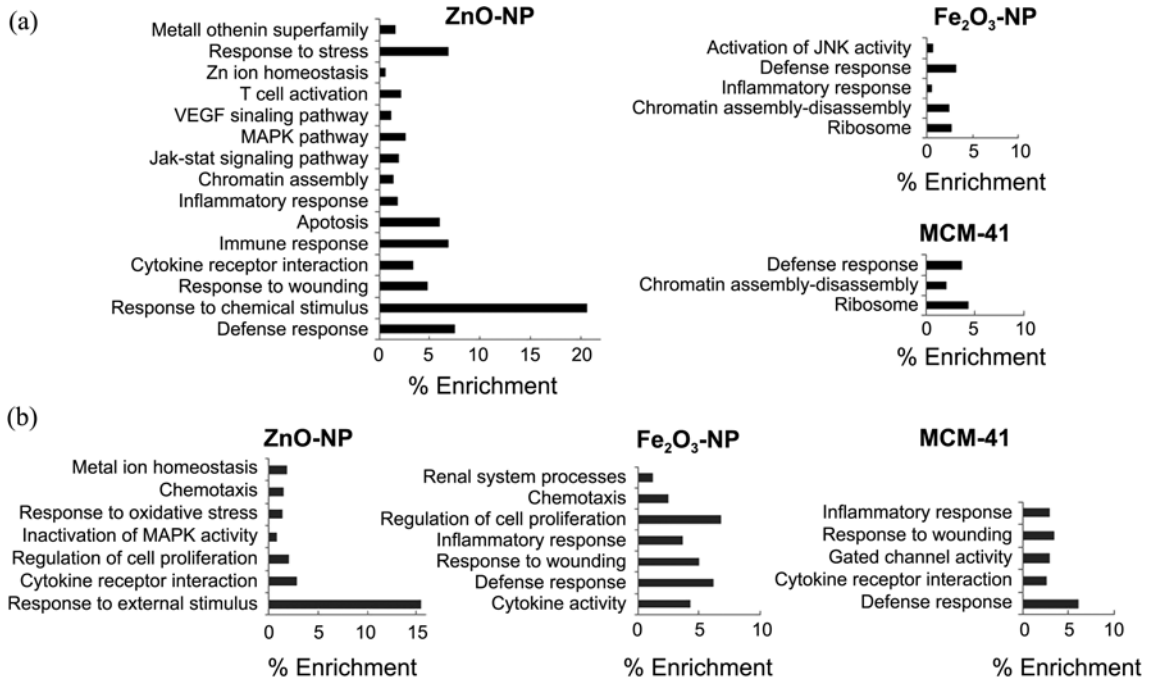

Figure 3. Categorization of greater than 2-fold altered genes on the basis of their gene ontology. (a) up-regulated (b) and down-regulated. Each bar represents the percent enrichment of the GO term against total altered genes as background.

silver NPs were shown to induce the expression of metallothionein genes in liver cells.[36] Most of the studies conducted with ZnO-NPs suggest that ZnO-mediated toxicity is primarily a result of oxidative stress and the generation of ROS.[19] In our study, in addition to the up-regulation of metallothioneins, we also observed reductions in eosinophil peroxidase and superoxide dismutase 2 mitochondrial (MnSOD) levels. Superoxide dismutase converts superoxide anion to hydrogen peroxide. In renal diseases, polycystic kidney damage oxidative stress and synthesis of H_2O_2 results in reduced mRNA levels of important antioxidant enzymes including MnSOD.[37] Reduction of mitochondrial SOD in our study suggests that upon prolonged exposure to ZnO NPs, the antioxidant activities of cells were compromised, which would further potentiate its toxicity. The findings of our study are also in agreement with earlier reports on ZnO-NPs in which similar changes in SOD expression and eosinophil peroxide transcription were observed.[17,19] We also observed induction of genes involved in Ca^{2+} homeostasis, namely protein kinase C gamma, S100 calcium binding protein, calbindin2, to name a few (Table S1). Some signaling pathways were also up regulated in ZnO-NPs treated samples, namely MAPK, Jak-Stat and VEGF signaling pathways.

Real Time PCR Validation of Key Toxicity Associated Genes. Based on the microarray expression changes and Gene Ontology search, eight genes that were up-regulated and associated with cellular toxicity were validated by real-time PCR. Among these, four genes, heat shock protein 6 (HSPA6), matrix metalloprotease 1 (MMP1), and pregnancy specific beta1 glycoprotein (PSG1, PSG9), showed more than 1.5-fold induction by all three NPs in the microarray analysis. Of the remaining four genes, chemokine C-C motif receptor 15 (CCL15) showed Fe_2O_3 and MCM-41 specific up-regulation, while v-fos fbj murine osteosarcoma viral oncogene homolog (vFOS fbj) was strongly induced by ZnO and to a lesser extent by Fe_2O_3. The interleukin17f (IL17f) and metallothionein 2a genes were specifically induced by ZnO. The fold changes in expressions of these genes obtained from microarray analysis are provided in Table S1. For all genes tested, the general dose response trends observed with real time PCR were consistent with microarray analyses (Fig. 4). However, in some cases the magnitude of fold induction seen in real-time PCR was higher than measured by microarray analysis, which was expected, as the dynamic range afforded by microarray is comparatively much lower. Only in the case of HSPA6 did we find that the microarray results were much higher than the actual changes in gene expression. Altogether, the results of real time PCR validation were in agreement with the microarray data, suggesting that the all three test materials induced expression of toxicity-associated genes. However, in comparison to Fe_2O_3 and MCM-41, ZnO exposure showed greater changes in expression, both in number and magnitude.

In conclusion, the data clearly show that although these three oxide NPs cause toxicity in cells, ZnO-NPs-mediated toxicity is much higher than those of MCM-41 and Fe_2O_3. Levels of cytotoxic response were observed in the following order: MCM-41 < Fe_2O_3-NPs < ZnO-NP. Gene ontology enrichment suggests that MCM-41 and Fe_2O_3 exposure, even at the concentrations used for various biomedical applications lead to toxic phenotypes in cells which can be classified as early response of cells towards environmental stressor. Although MCM-41 appeared to have marginal toxi-

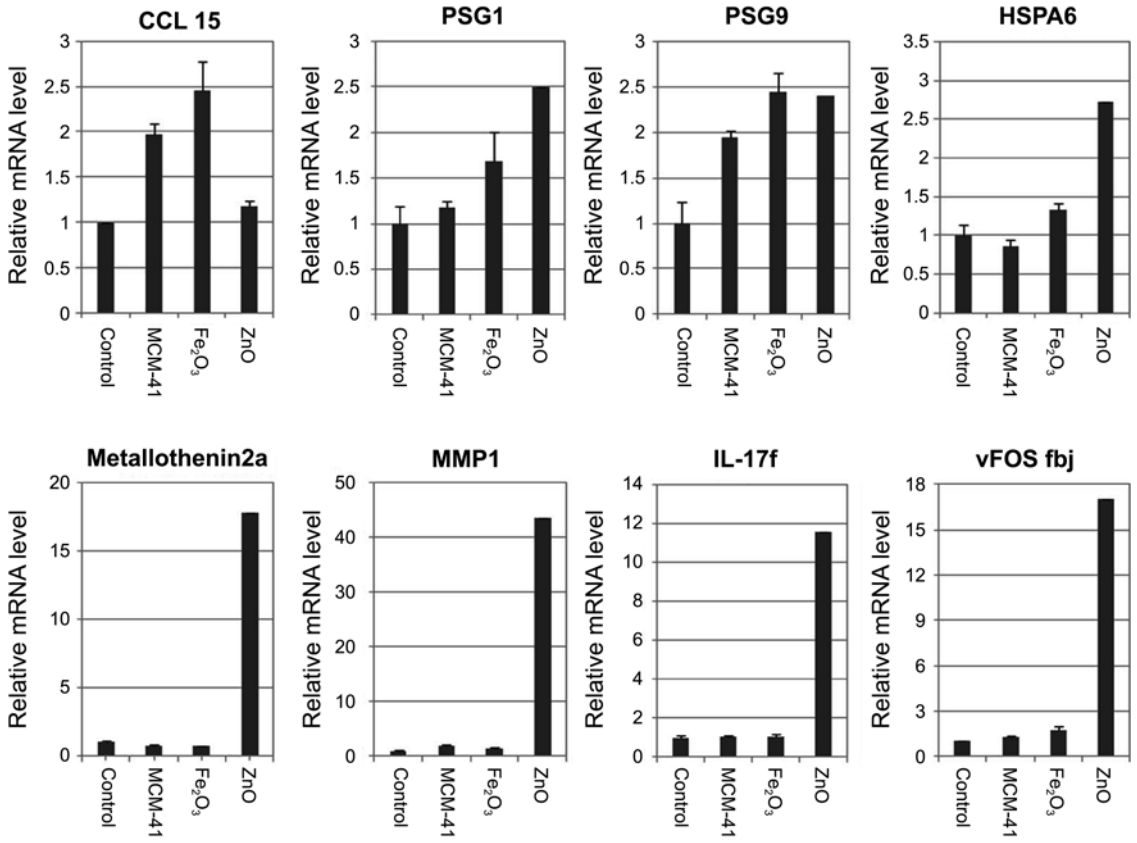

Figure 4. Real time PCR validation of selected genes that were found to be induced by NP exposure and have associations with toxic responses in the cells.

city, Fe_2O_3-NP-mediated alteration in gene expression implies toxicity above threshold levels, which the cell may or may not overcome depending upon the duration of exposure and the cell type. ZnO, even at lower concentrations, can induce substantial toxic responses in cells that are sufficient to trigger programmed cell death; hence, the use of ZnO for human applications should be scrutinized to establish safe levels prior to use. Therefore, our study shows that these NPs are more biologically challenging than originally thought. Further studies are needed to understand shape/size dependent cellular effects and the effects of surface modifications in overcoming these toxicity issues in order to provide a safe window for their end use.

Acknowledgments. This work was supported by a grant from the Ministry of Environment Eco-Technopia 21 Project (091-081-073) to D.-k. Lee. P.D. acknowledges support from the Sungkyunkwan University Post-Doctoral Fellowship in 2008.

References

1. Rothen-Rutishauser, B. M.; Schurch, S.; Haenni, B.; Kapp, N.; Gehr, P. *Environ. Sci. Technol.* **2006**, *40*, 4353-4359.
2. Huang, X.; Teng, X.; Chen, D.; Tang, F.; He, J. *Biomaterials* **2010**, *31*, 438-448.
3. Tang, J.; Xiong, L.; Wang, S.; Wang, J.; Liu, L.; Li, J.; Yuan, F.; Xi, T. *J. Nanosci. Nanotechnol.* **2009**, *9*, 4924-4932.
4. Oberdorster, G.; Elder, A.; Rinderknecht, A. *J. Nanosci. Nanotechnol.* **2009**, *9*, 4996-5007.
5. Long, T. C.; Saleh, N.; Tilton, R. D.; Lowry, G. V.; Veronesi, B. *Environ. Sci. Technol.* **2006**, *40*, 4346-4352.
6. Ji, L. L.; Chen, Y.; Wang, Z. T. *Exp. Toxicol. Pathol.* **2008**, *60*, 87-93.
7. Florea, A. M.; Splettstoesser, F.; Busselberg, D. *Toxicol. Appl. Pharmacol.* **2007**, *220*, 292-301.
8. Tao, Z.; Toms, B. B.; Goodisman, J.; Asefa, T. *Chem. Res. Toxicol.* **2009**, *22*, 1869-1880.
9. Di Pasqua, A. J.; Sharma, K. K.; Shi, Y. L.; Toms, B. B.; Ouellette, W.; Dabrowiak, J. C.; Asefa, T. *J. Inorg. Biochem.* **2008**, *102*, 1416-1423.
10. Huang, D. M.; Chung, T. H.; Hung, Y.; Lu, F.; Wu, S. H.; Mou, C. Y.; Yao, M.; Chen, Y. C. *Toxicol. Appl. Pharmacol.* **2008**, *231*, 208-215.
11. Fisichella, M.; Dabboue, H.; Bhattacharyya, S.; Saboungi, M. L.; Salvetat, J. P.; Hevor, T.; Guerin, M. *Toxicol. In Vitro* **2009**, *23*, 697-703.
12. Laaksonen, T.; Santos, H.; Vihola, H.; Salonen, J.; Riikonen, J.; Heikkila, T.; Peltonen, L.; Kumar, N.; Murzin, D. Y.; Lehto, V. P.; Hirvonen, J. *Chem. Res. Toxicol.* **2007**, *20*, 1913-1918.
13. Alexiou, C.; Jurgons, R.; Schmid, R.; Erhardt, W.; Parak, F.; Bergemann, C.; Iro, H. *Hno.* **2005**, *53*, 618-622.
14. Berry, C. C.; Wells, S.; Charles, S.; Curtis, A. S. *Biomaterials* **2003**, *24*, 4551-4557.
15. Brunner, T. J.; Wick, P.; Manser, P.; Spohn, P.; Grass, R. N.; Limbach, L. K.; Bruinink, A.; Stark, W. J. *Environ. Sci. Technol.* **2006**, *40*, 4374-4381.
16. Bregoli, L.; Chiarini, F.; Gambarelli, A.; Sighinolfi, G.; Gatti, A. M.; Santi, P.; Martelli, A. M.; Cocco, L. *Toxicology* **2009**, *262*, 121-129.

17. Kennedy, I. M.; Wilson, D.; Barakat, A. I. *Res. Rep. Health Eff. Inst.* **2009**, 3-32.
18. Karlsson, H. L.; Cronholm, P.; Gustafsson, J.; Moller, L. *Chem. Res. Toxicol.* **2008**, *21*, 1726-1732.
19. Huang, C. C.; Aronstam, R. S.; Chen, D. R.; Huang, Y. W. *Toxicol. In Vitro* **2009**.
20. Deng, X.; Luan, Q.; Chen, W.; Wang, Y.; Wu, M.; Zhang, H.; Jiao, Z. *Nanotechnology* **2009**, *20*, 115101.
21. Sharma, V.; Shukla, R. K.; Saxena, N.; Parmar, D.; Das, M.; Dhawan, A. *Toxicol. Lett* **2009**, *185*, 211-218.
22. Hong, S. W.; Hong, S. M.; Yoo, J. W.; Lee, Y. C.; Kim, S.; Lis, J. T.; Lee, D. K. *Proc. Natl. Acad Sci. USA* **2009**, *106*, 14276-14280.
23. Dennis, G., Jr.; Sherman, B. T.; Hosack, D. A.; Yang, J.; Gao, W.; Lane, H. C.; Lempicki, R. A. *Genome. Biol.* **2003**, *4*, P3.
24. Gojova, A.; Guo, B.; Kota, R. S.; Rutledge, J. C.; Kennedy, I. M.; Barakat, A. I. *Environ. Health Perspect.* **2007**, *115*, 403-409.
25. Cho, W. S.; Duffin, R.; Poland, C. A.; Duschl, A.; Oostingh, G. J.; Macnee, W.; Bradley, M.; Megson, I. L.; Donaldson, K. *Nanotoxicology* **2011**.
26. Baek, Y. W.; An, Y. J. *Sci. Total Environ.* **2011**, *409*, 1603-1608.
27. Radu, D. R.; Lai, C. Y.; Jeftinija, K.; Rowe, E. W.; Jeftinija, S.; Lin, V. S. *J. Am. Chem. Soc.* **2004**, *126*, 13216-13217.
28. Slowing, II.; Vivero-Escoto, J. L.; Wu, C. W.; Lin, V. S. *Adv. Drug. Deliv. Rev.* **2008**, *60*, 1278-1288.
29. Smirnov, P.; Lavergne, E.; Gazeau, F.; Lewin, M.; Boissonnas, A.; Doan, B. T.; Gillet, B.; Combadiere, C.; Combadiere, B.; Clement, O. *Magn. Reson. Med.* **2006**, *56*, 498-508.
30. Smirnov, P.; Gazeau, F.; Lewin, M.; Bacri, J. C.; Siauve, N.; Vayssettes, C.; Cuenod, C. A.; Clement, O. *Magn. Reson. Med.* **2004**, *52*, 73-79.
31. Cross, S. E.; Innes, B.; Roberts, M. S.; Tsuzuki, T.; Robertson, T. A.; McCormick, P. *Skin Pharmacol. Physiol.* **2007**, *20*, 148-154.
32. Nohynek, G. J.; Lademann, J.; Ribaud, C.; Roberts, M. S. *Crit. Rev. Toxicol.* **2007**, *37*, 251-277.
33. Pardigol, A.; Forssmann, U.; Zucht, H. D.; Loetscher, P.; Schulz-Knappe, P.; Baggiolini, M.; Forssmann, W. G.; Magert, H. J. *Proc. Natl. Acad Sci. U S A* **1998**, *95*, 6308-6313.
34. Nishina, H. W. T.; Katada, T. *J. Biochem.* **2004**, *136*, 123-126.
35. Snyder, S. K.; Wessner, D. H.; Wessells, J. L.; Waterhouse, R. M.; Wahl, L. M.; Zimmermann, W.; Dveksler, G. S. *Am. J. Reprod. Immunol.* **2001**, *45*, 205-216.
36. Kawata, K.; Osawa, M.; Okabe, S. *Environ. Sci. Technol.* **2009**, *43*, 6046-6051.
37. Maser, R. L.; Vassmer, D.; Magenheimer, B. S.; Calvet, J. P. *J. Am. Soc. Nephrol.* **2002**, *13*, 991-999.